13. Koh, S., Sanders, K. & Ward, S. Spontaneous electrical rhythmicity in cultured interstitial cells of Cajal from the murine small intestine. *J. Physiol. (Lond.)* **513.1,** 203–213 (1998).
14. Publicover, N. G. in *Pacemaker Activity and Intercellular Communication* (ed. Huizinga, J. D.) 175–192 (CRC, Boca Raton, 1995).
15. Cousins, H. M., Edwards, F. R., Hirst, G. D. & Wendt, I. R. Cholinergic neuromuscular transmission in the longitudinal muscle of the guinea-pig ileum. *J. Physiol. (Lond.)* **471,** 61–86 (1993).
16. Horowitz, B., Ward, S. & Sanders, K. Cellular and molecular basis for electrical rhythmicity in gastrointestinal muscles. *Annu. Rev. Physiol.* **61,** 19–43 (1999).
17. Ozaki, H., Stevens, R. J., Blondfield, D. P., Publicover, N. G. & Sanders, K. M. Simultaneous measurements of membrane potential, cytosolic Ca^{2+}, and tension in intact smooth muscles. *Am. J. Physiol.* **260,** C917–925 (1991).
18. Holman, M. E. Membrane potentials recorded with high resistance microelectrodes and the effects of changes in ionic environment on the electrical and mechanical activity of the smooth muscle of the taenia coloi of the guinea pig. *J. Physiol. (Lond.)* **141,** 464–488 (1958).
19. Gillespie, J. S. Spontaneous mechanical and electrical activity of stretched and unstretched intestinal smooth muscle cells and their response to sympathetic nerve stimulation. *J. Physiol. (Lond.)* **162,** 54–75 (1962).
20. Smith, T. K., Reed, J. B. & Sanders, K. M. Interaction of two electrical pacemakers in muscularis of canine proximal colon. *Am. J. Physiol.* **252,** C290–299 (1987).
21. Costa, M. & Furness, J. B. The peristaltic reflex: an analysis of the nerve pathways and their pharmacology. *Naunyn Schmiedebergs Arch. Pharmacol.* **294,** 47–60 (1976).
22. Smith, T. K. & Robertson, W. J. Synchronous movements of the longitudinal and circular muscle during peristalsis in the isolated guinea-pig distal colon. *J. Physiol. (Lond.)* **506,** 563–577 (1998).
23. Smith, T. K. & McCarron, S. L. Nitric oxide modulates cholinergic reflex pathways to the longitudinal and circular muscle in the isolated guinea-pig distal colon. *J. Physiol. (Lond.)* **512,** 893–906 (1998).
24. Costa, M. & Furness, J. B. in *Mediators and Drugs in Gastrointestinal Motility I. Morphological Basis of Neurophysiological Control* (ed. Bertacchini, A.) 279–382 (Springer, Berlin, 1982).
25. Smith, T. K. & Furness, J. B. Reflex changes in circular muscle activity elicited by stroking the mucosa: an electrophysiological analysis in the isolated guinea-pig ileum. *J. Auton. Nerve Syst.* **25,** 205–218 (1988).
26. Tomita, T. Electrical responses of smooth muscle to external stimulation in hypertonic solution. *J. Physiol. (Lond.)* **183,** 450–468 (1966).
27. Burnstock, G. & Prosser, C. Conduction in smooth muscle, comparative electrical properties. *Am. J. Physiol.* **199,** 553 (1960).
28. Smith, T. K., Bornstein, J. C. & Furness, J. B. Convergence of reflex pathways excited by distension and mechanical stimulation of the mucosa onto the same myenteric neurons of the guinea pig small intestine. *J. Neurosci.* **12,** 1502–1510 (1992).

Acknowledgements. This work was supported by the National Institute of Diabetes and Digestive and Kidney Diseases.

Correspondence and requests for materials should be addressed to T.K.S. (e-mail: tks@physio.unr.edu).

Dendritic spine changes associated with hippocampal long-term synaptic plasticity

Florian Engert & Tobias Bonhoeffer

Max-Planck Institute of Neurobiology, Am Klopferspitz 18A, 82152 München-Martinsried, Germany

Long-term enhancement of synaptic efficacy in the hippocampus is an important model for studying the cellular mechanisms of neuronal plasticity, circuit reorganization, and even learning and memory[1]. Although these long-lasting functional changes are easy to induce, it has been very difficult to demonstrate that they are accompanied or even caused by morphological changes on the subcellular level. Here we combined a local superfusion technique[2,3] with two-photon imaging[4], which allowed us to scrutinize specific regions of the postsynaptic dendrite where we knew that the synaptic changes had to occur. We show that after induction of long-lasting (but not short-lasting) functional enhancement of synapses in area CA1, new spines appear on the postsynaptic dendrite, whereas in control regions on the same dendrite or in slices where long-term potentiation was blocked, no significant spine growth occurred.

We used a local superfusion technique[2,3] to investigate whether long-term potentiation (LTP) of synaptic efficacy is accompanied by subcellular morphological changes. This allowed us to restrict synaptic activity and thus the site of LTP induction to a small region on the dendrite of the postsynaptic neuron. After a pyramidal neuron in area CA1 of a hippocampal slice culture was impaled with an intracellular recording electrode (resting potential of less than −65 mV) and filled with the fluorescent dye calcein, we evoked excitatory postsynaptic potentials (EPSPs) by electrical stimulation of the Schaffer collaterals (Fig. 1a). We then blocked transmitter release everywhere but in a small area of roughly 30 μm diameter, in which the blocking solution (10 μM Cd^{2+}, 0.8 mM Ca^{2+}) was displaced by 'normal' superfusion solution (Fig. 1b; see Methods). After we had identified an area with a suitable group of synapses, baseline synaptic transmission was recorded. We then induced LTP by pairing postsynaptic depolarizations with single presynaptic stimuli. Before, during and after the pairing, we used a two-photon laser-scanning microscope to acquire high-resolution three-dimensional image stacks of the postsynaptic neuron (Fig. 1c) with a frequency of usually six stacks per hour. Figure 2 shows a representative example of a dendritic branch located under the superfusion spot before, during and after the induction of LTP. The electrophysiological record (Fig. 2a) demonstrates the enhance-

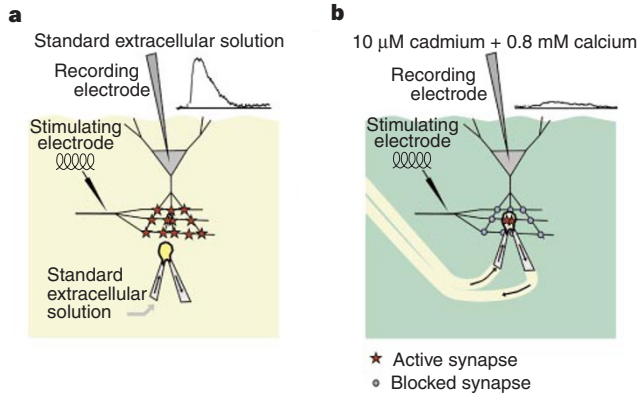

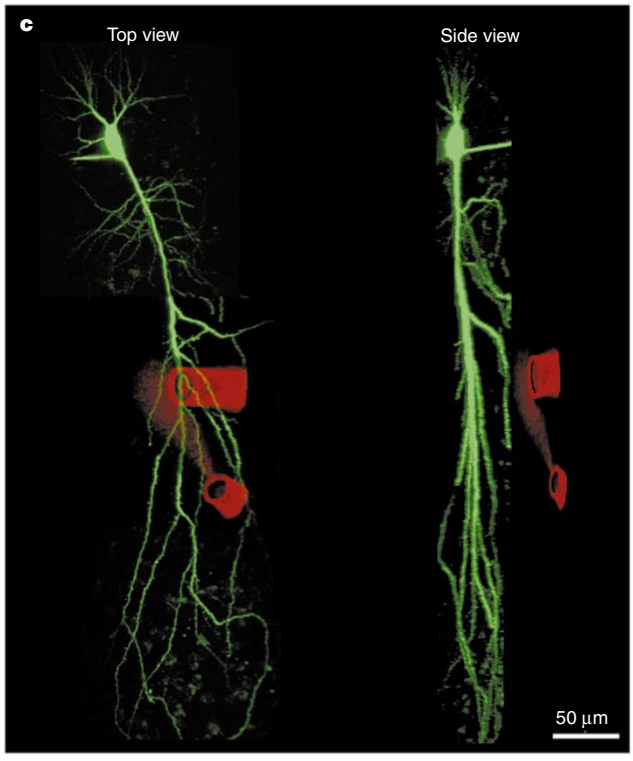

Figure 1 Experimental setup. **a**, **b**, Drawing of the recording situation. Actual EPSPs are shown as insets in the top right-hand corners. Active synapses are depicted as red stars, synapses blocked by 10 μM Cd^{2+} and low Ca^{2+} as blue dots. **c**, Two-photon laser-scanning image of a CA1 pyramidal neuron with the superfusion spot and the two pipettes (imaged on a different channel of the microscope with phase-contrast illumination) superimposed in false colours. Left, a maximum intensity projection through the complete picture stack; right, the same stack rotated by 90°. Only the dendritic branch that extends up to the surface of the slice is reached by the superfusion spot.

ment of synaptic strength. The columns of pictures for the different time points show the dendrite of interest from three different viewing angles (Fig. 2b). Clearly, two spines appear after synaptic enhancement in the positions marked with arrowheads. No spines can be seen at these positions in the rotated images of the first column, indicating that the appearance of spines cannot be attributed to a rotation artefact.

The raw data ('maximum intensity projection') of this (Fig. 3a) and the six remaining experiments in which LTP was successfully induced are shown in Fig. 3. In the first column, red dots on the neuron show the positions at which new spines grew, and blue dots denote where spines were found to disappear (see Methods, Blind evaluation). New spines usually appeared only under the superfusion spot (green overlay). Disappearing spines (blue dots) are seen more rarely, but at all locations. The panels to the right show magnifications of the regions of interest at −10, +30 and +60 min, and at an additional variable time point relative to LTP induction, as well as the electrophysiological data.

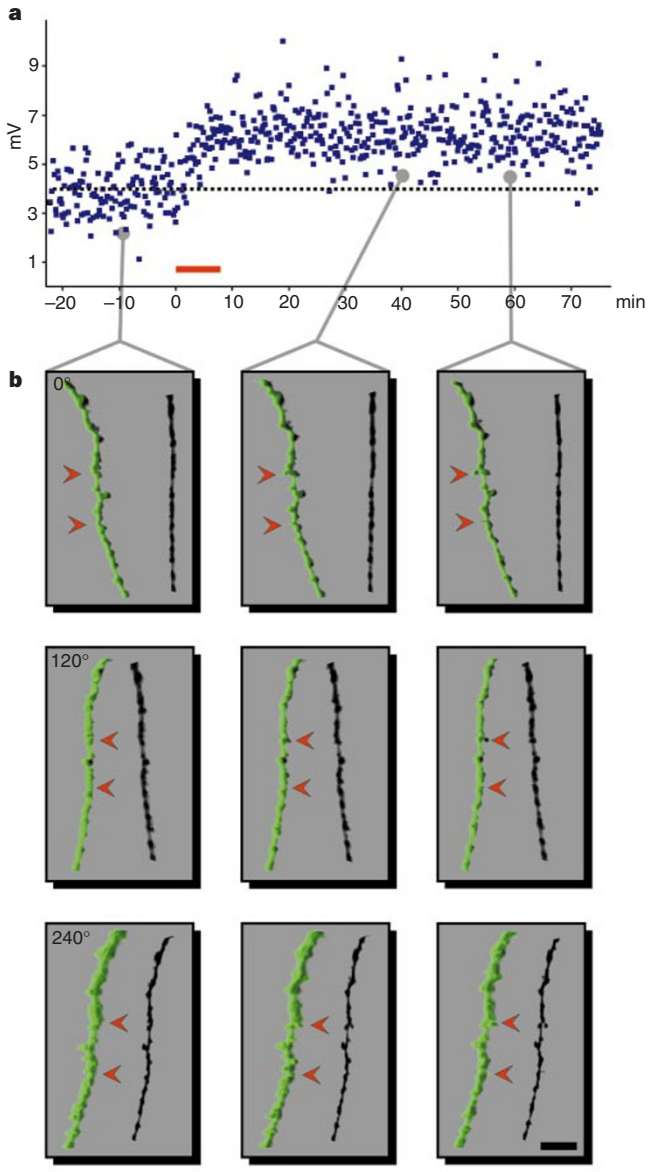

Figure 2 New spines emerge after the induction of LTP. **a**, Raw electrophysiological data. EPSP amplitudes of a pharmacologically isolated group of synapses are shown over time. After the pairing protocol, which was applied at the time indicated by the red bar, a stable and long-lasting potentiation of synaptic efficacy can be observed. **b**, Three columns of pictures taken at the time points indicated by the grey lines show a stretch of dendrite within the superfused region 'volume-rendered' from three different viewing angles (0°, 120° and 240°). A set of spines appears roughly 30 min after LTP induction at the sites marked by red arrowheads. The volume-rendering from different perspectives shows that the spines had really appeared *de novo* and were not just hidden behind the dendrite in the initial pictures. Scale bar, 5 μm. For animated time-lapse data, see Supplementary Information.

Three different conditions were used as controls: (1) regions far outside the superfusion spot ('off spot') were scrutinized for morphological changes. Apart from one case (Table 1), we saw no new spines in these areas (an example is shown in Fig. 4a), while disappearing spines were still observed; (2) experiments in which the induction of LTP was prevented by the NMDA (*N*-methyl-D-aspartate)-receptor antagonist D,L-2-amino-5-phosphonovalerate (AP5, 50 μM); and (3) experiments in which the pairing procedure did not result in a stable potentiation were analysed. In the last two cases, we never observed new spines after the pairing (Table 1 and Fig. 4b, c) but spines still disappeared in 'random' locations (Table 1). Perhaps the most interesting control is one case in which the pairing resulted only in a short potentiation of synaptic efficacy (<30 min; data not shown). Also here we did not observe any new spines.

For an unbiased analysis, an independent, 'blind' observer (see Methods) inspected the image stacks 'section by section' for microscopic morphological changes in the imaged neuron. In every experiment in which LTP was successfully induced ($n = 7$), the blind observer detected between two and nine new spines in the region underneath the superfusion spot (Table 1, LTP). We quantified the emergence or disappearance of spines by calculating the spine density on a length of dendrite (spines per 100 μm) before and after the induction procedure (Table 1). Although most spines remained stable, dendrites located under the superfusion spot showed a highly significant correlation between the appearance of new spines and an increase in synaptic efficacy (Fig. 5, red bars; Table 1; $P < 0.001$, two-tailed Students *t*-test). The disappearance of spines, on the other hand, was slightly anticorrelated with the successful induction of LTP (Fig. 5, blue bars; $P < 0.05$, two-tailed Students *t*-test).

Activity-related changes in dendritic structure and spine density have been examined in several preparations, but most of these studies have focused on long-term changes over several days to months[5–8]. Whether rapid changes in synaptic efficacy, such as those in LTP or LTD, are also accompanied by structural modifications is still a controversial question[9–12]. The general difficulty linked to this issue is twofold: first, the exact spatial location of the synapses in which LTP is induced is usually not known, so thousands of spines have to be investigated[6,10]; and second, statistical comparison of treated with untreated preparations requires a very large sample number to tease out the relatively small morphological changes[6]. A

Table 1 Statistics of the complete data set

Type of experiment	LTP	AP5	no LTP	'off spot'
Number of experiments	7	3	2	3
Length of dendrite examined (μm)	537	468	329	2,093
Spines counted	216	211	182	1,052
Spines per dendrite (μm^{-1})	0.40	0.45	0.55	0.50
New spines	32	0	0	4
100 × new spines per dendrite (μm^{-1})	6.0	0	0	0.2
Lost spines	1	11	0	26
100 × lost spines per dendrite (μm^{-1})	0.2	2.3	0	1.2

The first column shows data from experiments in which LTP was induced successfully. The last three columns show data from three different controls: block of LTP by the NMDA-antagonist AP5; unsuccessful pairing (no LTP); and data from outside the superfusion spot ('off spot'). For calculation of the lengths of dendrites the third dimension of the picture stack was taken into consideration; that is only the superficial 30 μm were ascribed to the LTP group whereas the rest of each respective experiment was pooled with the 'off spot' control (see Methods). Note that there are only four 'inappropriate' new spines in the off-spot column which were detected by the blind observer in a small cluster in only one of the experiments.

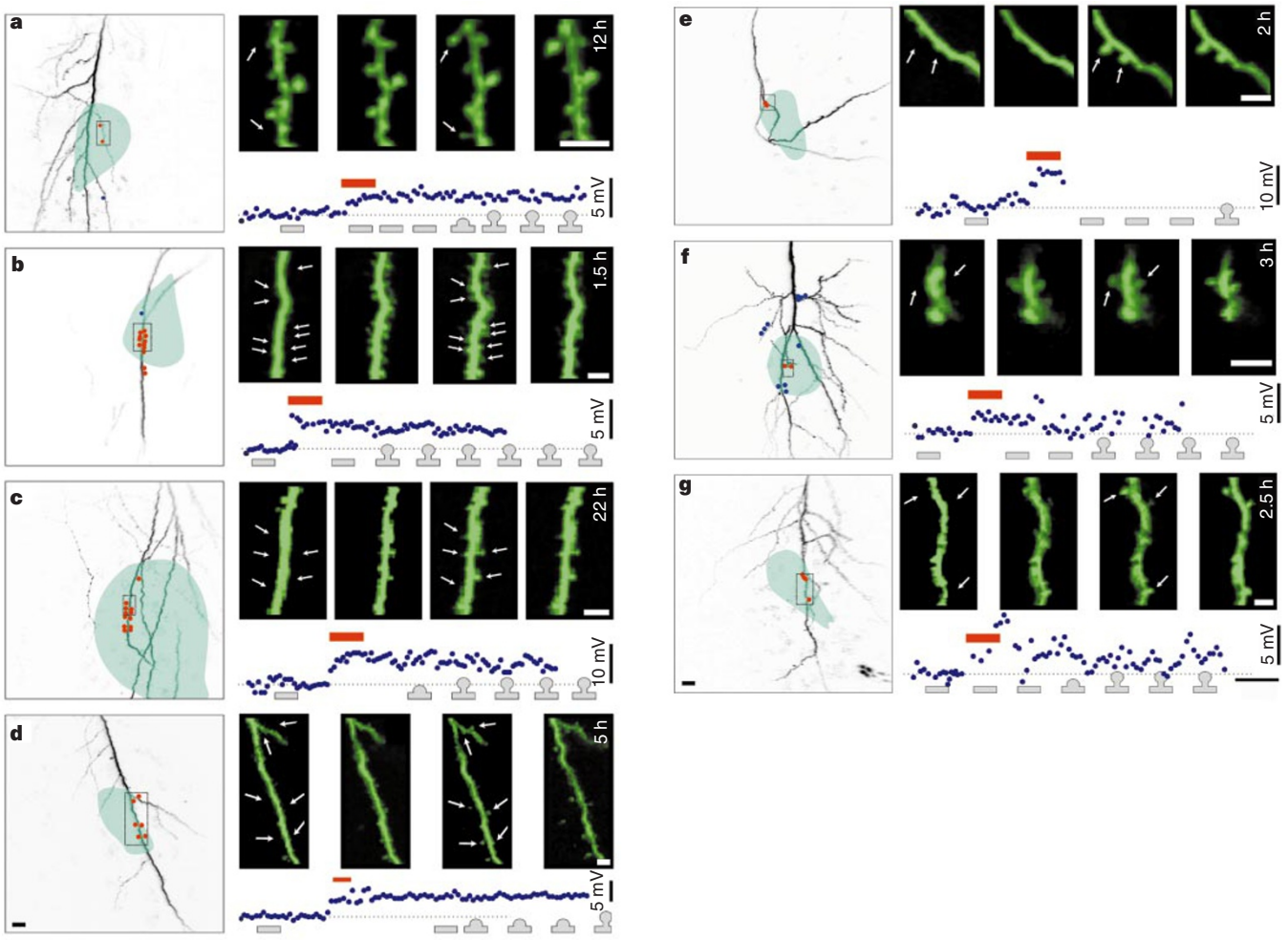

Figure 3 Experiments that produced a change in synaptic efficacy. **a**–**g**, Complete data set of experiments. The first experiment (**a**) is the same as that shown in Fig. 2. Left, a 170 μm × 170 μm maximum intensity projection of part of the dendrite is shown with the superfusion spot superimposed in false colour. Red dots denote the points where new spines were found to emerge; blue dots show points where spines disappeared. Note that the disappearing spines in **f** are located deep in the slice culture (>50 μm) and therefore stem from an 'off-spot' region. The first three right-hand columns show the magnified area of interest (dashed rectangle) at three time points: −10, +30 and +60 min; the last shows varying later time points as indicated in the panels (up to 22 h). White arrows indicate positions at which new spines were detected by blind analysis. They are only displayed in the first and third panels, which show the data used for the blind analysis. Below the four panels, electrophysiological data from the respective experiments are shown: five consecutive responses were averaged, and baseline levels are indicated by the dashed line and the pairing procedure by a red bar. Below the electrophysiological data, icons are shown at the times at which image stacks were acquired. The shape of the icon indicates whether new spines were detected. Scale bars for the morphological data: black, 10 μm; white, 3 μm. For animated time-lapse data of **d**, **e** and **g**, see Supplementary Information.

further complication is that if positive and negative changes happen simultaneously, as we show they do, and if they occur with about the same frequency, both kinds of change will go undetected. Therefore, the combination of the local superfusion technique (reducing the potential area for morphological changes to a region of approximately 30 μm diameter) and two-photon laser scanning (reducing the phototoxic damage[4] and thus greatly facilitating observations in living tissue) was crucial for our ability to detect morphological changes associated with LTP.

It has been proposed that the strength of synapses is controlled by changes in spine shape[9–11,13–16], such as shortening and/or widening of the neck which would reduce its electrical resistance and thus increase synaptic efficacy[14]. The results presented here do not directly address this issue; rather, they demonstrate that the growth of entirely new spines correlates with the induction of LTP. We cannot rule out, however, that additional smaller changes in spine morphology below our spatial resolution may also co-vary with synaptic strength.

We also have no direct proof that the emerging spines contain active synapses. However, most of the spines on pyramidal cells contain a postsynaptic density[6,17]. It is therefore likely that, even if it is not present from the very beginning, ultimately a synapse will occupy a new spine. In any case, the first increase in synaptic strength cannot originate from newly grown spines, because these appear no earlier than 30 min after LTP induction. One possibility is that the initial physiological enhancement of synapses is only transient, and that it is later gradually replaced by the formation of new synaptic sites[18] which then permanently contribute to the strengthening of overall synaptic weight.

We found that the disappearance of spines is not, as is the case in LTP and spine growth, controlled in a specific and activity-dependent manner, but that it rather occurs more-or-less randomly in time and space. Theoretically, there must also be a negative mechanism for the regulation of spine density if spines are not to increase constantly in number over the lifetime of a neuron. Whether the disappearance of spines, and thus synaptic weakening, occurs in a specific activity-dependent manner or by general synaptic decay has been a matter of debate[19–21]. Our data support the latter, although we cannot rule out that other components, such as functional (rather than morphological) changes, are controlled in

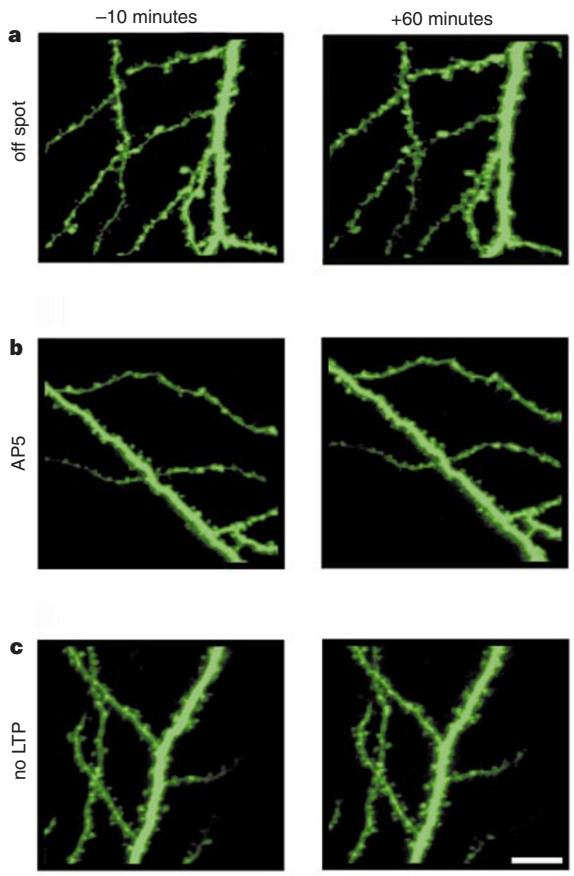

Figure 4. Control experiments. Three representative experiments with no change in synaptic efficacy. **a**, Images from a cell in which LTP was induced successfully, but the area shown is located well outside the superfused region (>150 μm). **b**, Data from one of the experiments in which LTP induction was blocked by AP5. **c**, Data from an experiment in which the induction of LTP was unsuccessful. The remaining controls are summarized in Fig. 5 and Table 1. Scale bar: 10 μm.

an activity-dependent way.

In summary, we have shown that the induction of LTP in the hippocampus results in the emergence of new spines. The most attractive explanation for this phenomenon is the formation of new synapses that appear within an hour of the initiating stimulus. Although more experiments are necessary on the precise nature of these changes, our results show that not only physiological but also structural changes are important when neurons change the efficacy of their connections.

Note added in proof: While this paper was in press, evidence for growth of new dendritic processes induced by strong synaptic activity was reported (M. Maletic-Savatic, R. Malinow and K. Svoboda, *Science* **283,** 1923–1927; 1999). Although addressing a slightly different question, the results are in line with our observations reported here. □

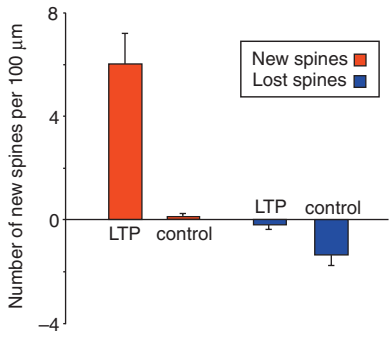

Figure 5 Quantitative results. The appearance and disappearance of spines was normalized to the complete length of examined dendrite in each individual neuron and the pooled results are plotted as the number of spines per 100 μm of dendrite. For the calculation of the results for the control group, data were pooled from experiments in which LTP was blocked by AP5, LTP induction had been unsuccessful, or regions remote from the superfusion spot were chosen (Table 1). Error bars, standard errors of the mean.

Methods

Preparation of slice cultures. Organotypical slice cultures of rat hippocampus were prepared as described[22,23] and selected for recording after 2–4 weeks in culture. Slice cultures consisting of only one or a few cell layers were used because the penetration depth of the superfusion technique is not much more than ~30 μm and therefore impractical in acute brain slices.

Data acquisition. Intracellular recordings were performed using an Axo-Clamp-2B amplifier (Axon Instruments) in current-clamp configuration. Sharp electrodes were used to prevent 'run-down' of cells due to washout of intracellular factors. Data were digitally sampled at 5 kHz, low-pass filtered at 3 kHz, and stored and analysed with custom made LabView software (National Instruments) on a PC. In all electrophysiology figures the amplitude of the EPSP (in mV) is plotted over time. The maximal slope of EPSPs was also determined in all experiments and the results are virtually the same apart from an expected slightly increased scatter of the data points.

Local superfusion and electrophysiology. Slice cultures were placed in the recording chamber and a stimulating electrode was positioned in the Schaffer collaterals. We impaled a pyramidal cell in the CA1 region with a recording electrode containing 3M potassium acetate and the fluorescent molecule calcein. Only cells with resting potentials <–65 mV were used for further experimentation. After a stable response to Schaffer collateral activation was recorded, we bathed the slice culture in a solution containing a moderate dose of Cd^{2+} (10 μM) and a low concentration of Ca^{2+} (0.8 mM) to prevent presynaptic Ca^{2+} influx, thereby abolishing transmitter release and, consequently, all postsynaptic responses. A local superfusion system[2,3] containing normal extracellular solution (with a slightly elevated Ca^{2+} concentration[3] of 5 mM) was then employed to restore locally synaptic responses in a region with a diameter of ~30 μm. Using this technique, we 'searched' for synapses mediating responses from the stimulated Schaffer collaterals to the postsynaptically recorded neuron. After uncovering such a group of synapses, we recorded a baseline of the postsynaptic intracellular responses and acquired a first two-photon image of the filled neuron. After 10 min of baseline recording (0.1 Hz stimulation), synapses were enhanced by a pairing procedure (30 presynaptic stimuli concurrent with 1 nA postsynaptic current injections at an interstimulus interval of 10 s). Subsequently, EPSP amplitudes were recorded for up to 2 h until the electrode was withdrawn. After the removal of the electrode, the neuron could be observed for up to 28 h with the two-photon microscope.

Two-photon microscopy. A scanhead for confocal microscopy (Biorad 1024, Biorad) was modified for two-photon microscopy and equipped with a new photomultiplier (Hamamatsu Photonics) for external detection of fluorescent light. A 'Tsunami Lite' titanium-sapphire femtosecond laser pumped by a 'Millennia' neodymium yttrium vanadate solid-state laser (both SpectraPhysics) served as the two-photon light source. The scanhead was connected to a Zeiss Axiovert microscope and images were acquired with a resolution of 0.33 μm in the *x* and *y* directions and 1–1.8 μm in the z direction using a 63× Neofluar, oil-immersion objective. They were averaged between one and three times depending on the concentration of the fluorescent dye. The relatively large spacing in the *z*-direction was needed to achieve a time resolution of roughly one image per 10 min. Closer spacing would have resulted in too much laser power per unit time, causing noticeable photodynamic damage. It is conceivable that, because of the spacing, we missed the smallest spines, which might explain why the overall spine density was lower than that reported in the literature[8].

For volume rendering, we used the Imaris (BitPlane) raytrace-shadow projection algorithm on an SGI 02 (Silicon Graphics). No further filtering or deconvolution algorithms were applied.

The online 3D imaging of the neuron greatly facilitated the localization of

dendritic branches suitable for superfusion because it allowed us to select those synapses that were located close to the surface of the slice culture (Fig. 1c, right). When the dendrites were located more than 30 μm below the surface, no postsynaptic EPSP could be elicited ($n = 85$ experiments), indicating that this is the maximal penetration depth of the superficially applied superfusion spot. Thus for further analysis, only parts of the dendrite closer than 30 μm to the surface were considered to be potential sites of active synapses.

Blind evaluation. The data were blindly evaluated by an observer who was not familiar with the experiments and not directly involved in the study. The observer was confronted with pairs of data sets (before and 1 h after pairing). These data sets included: (1) all experiments in which pairing had successfully induced LTP (7 experiments); (2) those experiments in which pairing was applied but LTP was prevented by 50 μM AP5 (3 experiments); (3) three pairs of data sets that came from successful experiments but were from parts of the dendrite where activity was blocked and where therefore no changes were expected; and (4) two pairs of data sets in which the pairing procedure did not result in a long-lasting potentiation. The observer received the original data sets (stacks of images) and carefully compared spines before and after pairing by screening through the individual 'sections' using the 'Confocal Assistant' software (Biorad). All spines were labelled and given a rating between one (barely visible) and three (head and neck clearly distinguishable). After complete evaluation, the code was broken and (2), (3) and (4) were pooled into a 'control' group. To reduce the noise in this procedure, only spines with a difference in the above rating greater than one ($\Delta > 1$) between the two time frames were considered to be appearing or vanishing spines. They were entered into the statistics and plotted as red (or blue) dots on a picture of the dendritic tree which was overlayed with the superfusion spot (Fig. 3). To correct for the length of dendrite examined in each experiment, a weighted average was used to calculate the means and *t*-values. We also verified that including smaller changes in spine morphology ($\Delta = 1$) in the analysis did not change the basic results.

Received 22 February; accepted 7 April 1999.

1. Bliss, T. V. P. & Collingridge, G. L. A synaptic model of memory: long-term potentiation in the hippocampus. *Nature* **361,** 31–39 (1993).
2. Veselovsky, N. S., Engert, F. & Lux, H. D. Fast local superfusion technique. *Pflügers Arch.* **432,** 351–354 (1996).
3. Engert, F. & Bonhoeffer, T. Synapse specificity of long-term potentiation breaks down at short distances. *Nature* **388,** 279–284 (1997).
4. Denk, W., Strickler, J. H. & Webb, W. W. Two-photon laser scanning fluorescence microscopy. *Science* **248,** 73–76 (1990).
5. Woolley, C. S., Gould, E., Frankfurt, M. & McEwen, B. S. Naturally occurring fluctuation in dendritic spine density on adult hippocampal pyramidal neurons. *J. Neurosci.* **10,** 4035–4039 (1990).
6. Moser, M.-B., Trommald, M. & Andersen, P. An increase in dendritic spine density on hippocampal CA1 pyramidal cells following spatial learning in adult rats suggests the formation of new synapses. *Proc. Natl Acad. Sci. USA* **91,** 12673–12675 (1994).
7. Collin, C., Miyaguchi, K. & Segal, M. Dendritic spine density and LTP induction in cultured hippocampal slices. *J. Neurophysiol.* **77,** 1614–1623 (1997).
8. McKinney, R. A., Capogna, M., Dürr, R., Gähwiler, B. H. & Thompson, S. M. Miniature synaptic events maintain dendritic spines via AMPA receptor activation. *Nature Neurosci.* **2,** 44–49 (1999).
9. Desmond, N. L. & Levy, W. B. Morphological correlates of long-term potentiation imply the modification of existing synapses, not synaptogenesis, in the hippocampal dentate gyrus. *Synapse* **5,** 139–143 (1990).
10. Hosokawa, T., Rusakov, D. A., Bliss, T. V. P & Fine, A. Repeated confocal imaging of individual dendritic spines in the living hippocampal slice: Evidence for changes in length and orientation associated with chemically induced LTP. *J. Neurosci.* **15,** 5560–5573 (1995).
11. Buchs, P. A. & Muller, D. Induction of long-term potentiation is associated with major ultrastructural changes of activated synapses. *Proc. Natl Acad. Sci. USA* **93,** 8040–8045 (1996).
12. Sorra, K. E. & Harris, K. M. Stability in synapse number and size at 2 hr after long-term potentiation in hippocampal area CA1. *J. Neurosci.* **18,** 658–671 (1998).
13. Crick, F. Do dendritic spines twitch? *Trends Neurosci.* **5,** 44–46 (1982).
14. Svoboda, K., Tank, D. W. & Denk, W. Direct measurement of coupling between dendritic spines and shafts. *Science* **272,** 716–719 (1996).
15. Fischer, M., Kaech, S., Knutti, D. & Matus, A. Rapid actin-based plasticity in dendritic spines. *Neuron* **20,** 847–854 (1998).
16. Dunaevsky, A., Heintz, N., Mason, C. A. & Yuste, R. Two-photon imaging of dendritic spines of cerebellar and cortical cells transfected with GFP. *Soc. Neurosci. Abstr.* **24,** 316.1 (1998).
17. Gray, E. G. Electron microscopy of synaptic contacts on dendritic spines of the cerebral cortex. *Nature* **183,** 1592–1593 (1959).
18. Bolshakov, V. Y., Golan, H., Kandel, E. R. & Siegelbaum, S. A. Recruitment of new sites of synaptic transmission during the cAMP-dependent late phase of LTP at CA3–CA1 synapses in the hippocampus. *Neuron* **19,** 635–651 (1997).
19. Bienenstock, E. L., Cooper, L. N. & Munro, P. W. Theory for the development of neuron selectivity: orientation specificity and binocular interaction in visual cortex. *J. Neurosci.* **2,** 32–48 (1982).
20. Miller, K. D. & MacKay, D. C. The role of constraints in Hebbian learning. *Neural Comput.* **6,** 100–126 (1994).
21. Turrigiano, G. G., Leslie, K. R., Desai, N. S., Rutherford, L. C. & Nelson, S. B. Activity-dependent scaling of quantal amplitude in neocortical neurons. *Nature* **391,** 892–896 (1998).
22. Gähwiler, B. H. Organotypic monolayer cultures of nervous tissue. *J. Neurosci. Meth.* **4,** 329–342 (1981).
23. Bonhoeffer, T., Staiger, V. & Aertsen, A. Synaptic plasticity in rat hippocampal slice cultures: Local 'Hebbian' conjunction of pre- and postsynaptic stimulation leads to distributed synaptic enhancement. *Proc. Natl Acad. Sci. USA* **86,** 8113–8117 (1989).

Supplementary information is available on *Nature*'s World-Wide Web site (http://www.nature.com).

Acknowledgements. We thank I. Kehrer for help with the evaluation of the data, and M. Hübener, M. Korte and M. Meister for comments on the manuscript.

Correspondence and requests for materials should be addressed to T.B.

A family of mammalian Na^+-dependent L-ascorbic acid transporters

Hiroyasu Tsukaguchi*†, Taro Tokui*†‡, Bryan Mackenzie*†, Urs V. Berger*, Xing-Zhen Chen*, Yangxi Wang*, Richard F. Brubaker§ & Matthias A. Hediger*‖

* *Membrane Biology Program and Renal Division, Department of Medicine, Brigham & Women's Hospital and Harvard Medical School, and*
‖ *Department of Biological Chemistry & Molecular Pharmacology, Harvard Medical School, 77 Avenue Louis Pasteur, Boston, Massachusetts 02115, USA*
§ *Department of Ophthalmology, Mayo Clinic, 200 First Street Southwest, Rochester, Minnesota 55905, USA*
† *These authors contributed equally to this work.*

Vitamin C (L-ascorbic acid) is essential for many enzymatic reactions, in which it serves to maintain prosthetic metal ions in their reduced forms (for example, Fe^{2+}, Cu^{+})[1,2], and for scavenging free radicals in order to protect tissues from oxidative damage[3]. The facilitative sugar transporters of the GLUT type can transport the oxidized form of the vitamin, dehydroascorbic acid[4–6], but these transporters are unlikely to allow significant physiological amounts of vitamin C to be taken up in the presence of normal glucose concentrations, because the vitamin is present in plasma essentially only in its reduced form[7]. Here we describe the isolation of two L-ascorbic acid transporters, SVCT1 and SVCT2, from rat complementary DNA libraries, as the first step in investigating the importance of L-ascorbic acid transport in regulating the supply and metabolism of vitamin C. We find that SVCT1 and SVCT2 each mediate concentrative, high-affinity L-ascorbic acid transport that is stereospecific and is driven by the Na^+ electrochemical gradient. Despite their close sequence homology and similar functions, the two isoforms of the transporter are discretely distributed: SVCT1 is mainly confined to epithelial systems (intestine, kidney, liver), whereas SVCT2 serves a host of metabolically active cells and specialized tissues in the brain, eye and other organs.

We isolated a 2,472-base-pair complementary DNA coding for a 604-amino-acid protein, SVCT1 (sodium-dependent vitamin C transporter 1), by screening a rat kidney cDNA library for Na^+-dependent L-[^{14}C]ascorbic acid transport activity in RNA-injected *Xenopus* oocytes (Fig. 1). Subsequent polymerase chain reaction (PCR)-based homology screening yielded a related cDNA (of 6.5 kilobases (kb), from rat brain) coding for a 592-amino-acid protein, SVCT2, with 65% amino-acid identity to SVCT1. SVCT1 and SVCT2 have similar hydropathy profiles, each predicting 12 putative membrane-spanning domains. SVCT2 is 84% identical (at the amino-acid level) to a predicted partial polypeptide encoded by the human *KIAA0238* gene[8]; therefore, KIAA0238 may be the species homologue of rat SVCT1. SVCT1 is 59% identical to KIAA0238 and 32% identical to a mouse yolk-sac permease-like molecule (mYspl1)[9] of unknown function. SVCT1 and SVCT2 share weak homology with putative permeases of *Caenorhabditis elegans* and *Arabidopsis thaliana*, and with a bacterial purine/pyrimidine permease[10]. We found no significant sequence homology between SVCT and any other known family of mammalian membrane transporters[11]; hence SVCT1 and

‡ Present address: Sankyo Company Ltd, Analytical and Metabolic Research Laboratories, 2-58 Hiromachi 1-Chome, Shinagawa-ku, Tokyo 140, Japan.